Proceedings of the International Gas Turbine Congress 2019 Tokyo
November 17-22, 2019, Tokyo, Japan

Impeller design and multi-stage architecture optimisation for turbocompressors operating with a helium-neon gas mixture

Maxime Podeur*[1], Damian M. Vogt[1], Sebastiano Mauri[2], Philipp Jenny[2]

[1]Institute of Thermal Turbomachinery (ITSM), University of Stuttgart, Pfaffenwaldring 6, Stuttgart 70550, Germany
[2]MAN Energy Solutions Schweiz AG

ABSTRACT

As part of the design of a new particle accelerator at CERN, a research is conducted to study the challenges and opportunities of multi-stage turbocompressor machines operating with light gases and more specifically with a mixture of helium and neon. First, a 1D stage performance prediction model is implemented and coupled with a genetic algorithm in order to generate an impeller database. Then, a stacking method is developed considering design philosophies and technological limitations observed in the industry. This model is coupled with a second loop of the same genetic algorithm, which provides multi-stage architectures optimised for either compactness, i.e. number of stages, or efficiency. For both objectives, an ideal number of stages can be determined which increases significantly as the operating gas becomes lighter. The impellers diversity within the database also plays an important role on the overall machine architecture. Finally, in alignment with potential technological improvements, the motor maximum rotational speed is varied to study the achievable reduction in the required number of stages.

NOMENCLATURE

A, B, C, D, H and G, n = coefficients in equation [-]
A_1 = inlet flow area [m^2]
a = speed of sound [m/s]
BL = blade loading [-]
D_2 = impeller tip diameter [m]
D_{1s} = impeller inlet shroud diameter [m]
D_{1h} = impeller inlet hub diameter [m]
Deq = diffusion factor [-]
h_2 = blade exit width [m]
k = impeller shape factor $\left(1-(D_{1h}/D_{1s})^2)\right)$ [-]
M_{U_2} = impeller tip Mach number $(U_2/\sqrt{\gamma RT_{t1}})$ [-]
$\dot{m}$ = mass flow rate [kg/s]
$\dot{V}_1$ = inlet volume flow rate [m^3/s]
OM = operating margin [-] $((\dot{m}_c-\dot{m}_s)/\dot{m}_c)$
P = pressure [Pa], penalty [-]
T = temperature [K], Tesla
U_2 = impeller tip speed [m/s]
xHe = mole fraction of helium [-]
Z = number of blades [-]

Greek Symbols

η = efficiency [-]
γ = isentropic exponent [-]
λ = work input coefficient $(\Delta h/U_2^2)$ [-]
Ω = rotational speed [RPM]
ψ = pressure rise coefficient $(\eta\lambda)$ [-]
ϕ_{t1} = inlet flow coefficient $(\dot{m}/\rho_{t1}D_2^2U_2)$ [-]
ϕ_2 = outlet flow coefficient (C_{m2}/U_2) [-]
Π = pressure ratio [-]

Subscripts

1 = impeller inlet
2 = impeller outlet
c = choke
d = design
high = high rotational speed
in = machine inlet
low = low rotational speed
obj = objective
opt = optimal
out = machine outlet
p = polytropic
req = required
red = reduced
ref = reference
s = surge

INTRODUCTION

The current research has been conducted within the framework of a European project coordinated by CERN in Geneva, Switzerland. As recently advertised, the research centre is currently designing a new particle accelerator aiming at higher energy of particle collision enabling to explore a new research space for the potential discovery of unknown particles. To do so, the perimeter of the accelerating loop as well as the magnetic field of the superconducting magnets are increased to 100 km and 16 T respectively in comparison to its predecessor, the so-called Large Hadron Collider (LHC) featuring a 27-km perimeter and superconducting magnets reaching a magnetic field of 8 T. A schematic of the Future Circular Collider (FCC) is shown in Figure 1 and compared to the actual LHC.

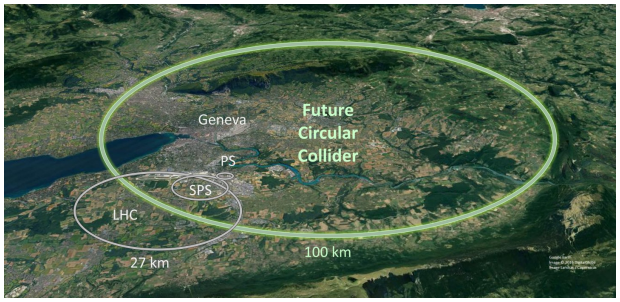

Fig.1 Scheme of the Future Circular Collider (FCC)

With this novel accelerator architecture, the heat load on the cryogenic cycle used to maintain the superconducting magnet near absolute 0 K is significantly increased in comparison to the LHC. One of the objectives of the FCC cryogenic cycle is thus to replace

ISBN978-4-89111-010-9

the original open loop pre-cooling cycle requiring a constant supply of LN_2 with a sustainable and efficient closed cycle with low acquisition, operating and maintenance cost.

To address this objective, one promising solution is to use a mixture of helium and neon, also called nelium, as the process gas. By adding neon, acting as a ballast gas, the use of multi-stage turbocompressor becomes economically more viable, especially when looking at the required number of stages. In fact, while standard cycles operating with pure helium use screw compressor with inherent low efficiencies to maintain the cost at a reasonable level, the addition of neon enables to reach higher overall machine efficiency and to increase significantly the maximum pressure ratio per turbocompressor stage. However, it is also worth noting that adding neon implies several drawbacks, the first one being the gas cost in comparison to a pure helium configuration. Secondly, when neon is added, the gas heat conductivity decreases and other components, which are part of the cryogenic cycle such as heat exchangers or cold box, become larger. Consequently, the manufacturing of these large components could become hindered or unaffordable. Finally, the theoretical maximal mole fraction of neon in the cycle is limited to 0.8 due to the presence of a liquid phase after the gas expansion for higher neon content. Nevertheless, the whole range of gas mixture, i.e. from pure helium to pure neon, is taken into consideration hereafter to study the effect of the widest diversity of fluid properties on the compressor architecture and performance.
The purpose of this paper is to focus on the compressor architecture rather than to analyse the effect of the gas mixture over the different cycle components. Hence, the following research aims at studying the effect of the gas mixture and the available impellers on multi-stage machine architecture. To do so, an optimisation algorithm is coupled with a model generating preliminary impeller geometries in order to build an impeller database. The same optimisation algorithm is subsequently coupled with a model predicting the performance of multi-stage machines. Finally, the database is used to obtain an optimised multi-stage architecture for specific boundary conditions.

In the literature, multiple references can be found to define geometries and assess performances of radial compressor stages such as Aungier [1], Lüdtke [2], Dixon [3], Casey and Rusch [4] or Dalbert et. al [6]. In parallel, challenges associated with the design of multi-stage architectures are also often described as in Lüdtke [2] or Dalbert et. al [7]. This study attempts to close the gap between these two research topics. Hence, instead of optimising each impeller of a specific multi-stage architecture by providing stage design parameters derived from the multi-stage machine operation (e.g. Al-Busaidi and Pilidis [8, 9], or Romei et. al [10]), an approach closer to the industry's ways of working is followed here. Therefore, an impeller database is first created and promising impellers are selected according to the needs determined during the elaboration of the multi-stage architecture. In fact, in the industry, new impellers cannot be optimised for each application. Thus, companies often have to rely on their existing impeller designs and adapt them by means of scaling or impeller trimming to fulfil the customer specifications.

The paper is organised as follows: Firstly, building on the described framework, potential challenges associated with the specific application under study are highlighted. The model predicting the stage performance as well as the stacking method evaluating the multi-stage machine performance are then introduced. This leads to the description of the optimisation algorithm coupled with these models. Finally, results of the study are presented for several variables such as design gas mixture, available impellers and potential technological improvements forecasted for the near future.

PROCEDURE

The boundary conditions required for the design of the multi-stage machine are directly derived from the particle accelerator operations. In fact, the heat load distribution on the cryogenic cycle can be estimated from machine operations as well as from the pre-cooling cycle architecture shown in Figure 2.

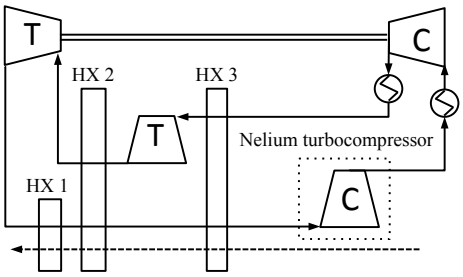

Fig.2 Nelium pre-cooling cryogenic cycle

Based on the pre-cooling cycle architecture and the proportion of helium and neon in the process gas, the mass flow rate, discharge pressure and gas inlet properties can be obtained at maximum load. These boundary conditions are provided in Figure 3 for different gas mixtures and will define the machine design point.

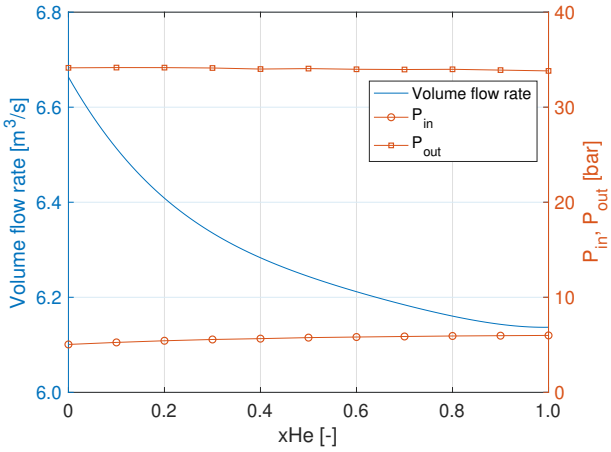

Fig.3 Design volume flow rate as well as compressor inlet and discharge pressure for the whole gas mixture range

In the following research, nelium is treated as a real gas. Hence, a table of required fluid properties is generated following mixing laws for a specific gas composition. Fluid properties are then interpolated depending on the gas static temperature and pressure. The models implemented have been validated using results from commercial software such as REFPROP and PPDS.

The wide variety of flow properties encountered in the whole range of gas mixtures is illustrated through the gas speed of sound distribution, here evaluated with an inlet stagnation temperature of 300 K and shown in Figure 4. The rapid evolution of the gas speed of sound directly influences the variation of impeller tip Mach numbers M_{U_2} and in turn the achievable pressure ratios. In fact, since neon and helium are both monoatomic gases, the achievable pressure ratio per stage is mainly governed by the tip Mach number. Hence, maximum pressure ratios can be derived from the impeller rotational speed threshold imposed by the motor and impeller manufacturing process or material. The maximum impeller pressure ratio evolution with respect to the mole fraction of helium is displayed on the same figure for an assumed polytropic efficiency of 0.85, a work input coefficient of 0.7 and an impeller tip rotational speed of 300 m/s. As illustrated, the strong change in gas proper-

ties and achievable pressure ratios directly impact the multi-stage machine architecture, and more specifically, the required number of stages. An initial trend for the latter can be estimated by assuming a constant pressure ratio per stage. As a result, the required number of stages is inversely proportional to the logarithm of the stage pressure ratio and thus rapidly increases towards high helium content.

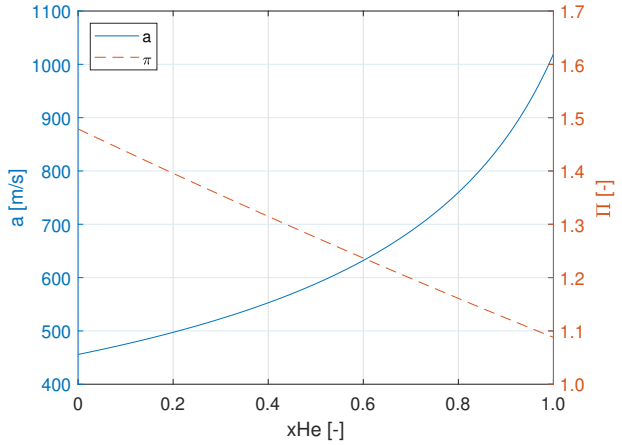

Fig.4 Gas speed of sound and impeller pressure ratio estimates for the whole gas mixture range and U_2 = 300 m/s

Moreover, designing a multi-stage machine for such light gases imposes several technical requirements, the first one being the sealing capability against these particularly low molecular weight gases. The second requirement is the need for high speed motors. As discussed above, given the high gas speed of sound, a certain impeller tip velocity is required to provide tip Mach numbers maximising the pressure ratio per stage. Hence, while rotational speed limitation for turbocompressors operating with heavier gas possibly comes from losses inherent to transonic conditions, the limitation in the case of light gases comes from either the maximum allowable motor speed or the material and manufacturing technique used. The last requirement is the capacity to stack a high number of stages on a single shaft with the same objective of reaching the highest pressure rise per machine.

For these reasons, the so-called HOFIM^{TM} (High-speed Oil-Free Integrated Motor-compressor) developed by MAN Energy Solutions was selected as a particularly suitable candidate for the baseline machine. This choice ensures that the subsequent architectures of multi-stage machines will follow the design boundaries encountered in the industry. Hence, technical limitations such as motor maximum speed, minimum shaft diameters and maximum impeller diameters are taken into account. Moreover, embedded experience in the machine rotor dynamics help to define a limitation for the maximum number of impellers per shaft. The HOFIM^{TM} comes either in single or tandem configuration for one or two casings respectively. Machines are then positioned in series with intercoolers in between, as illustrated in Figure 5.

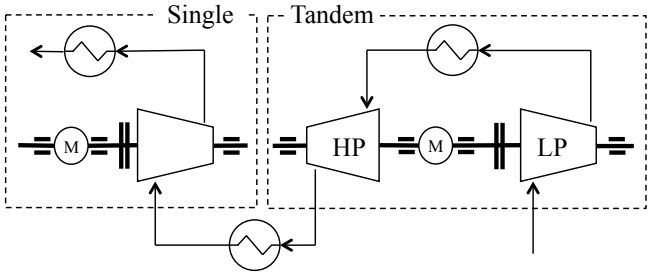

Fig.5 Single and tandem HOFIM^{TM} architecture

The objective of this study is to design several multi-stage machines, each of which is based on the HOFIM^{TM} architecture and optimised for different mixtures of helium and neon. To do so, a wide variety of design parameters enables to build a database of impellers, which could be required in the multi-stage machine later on. The architecture of the machine is then developed and optimised with respect to compactness, efficiency and range through a stacking method. The procedure described above is summarised in Figure 6.

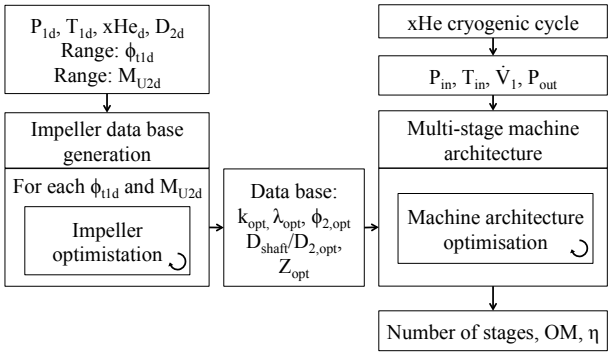

Fig.6 Overall procedure followed

1D MODEL

In order to generate the impeller geometries constituting the database, a 1D performance evaluation model has been implemented. The following boundary conditions are set for each impeller:

$$xHe_d = 0.5,\ P_{1d} = 1\ \text{bar},\ T_{1d} = 300\ \text{K and}\ D_{2d} = 450\ \text{mm}$$

Additional variable inputs include: the design inlet flow coefficient ϕ_{t1d}, the design impeller tip Mach number M_{U_2d}, the impeller shape factor k, the outlet flow coefficient ϕ_2, the work input coefficient λ, the ratio of shaft to impeller outlet diameter D_{shaft}/D_2 and the impeller blade number Z. All impellers are shrouded and their performance calculated for a vaned diffuser. The diffuser blade as well as the stage return channel geometry are however not estimated. The compressor impeller geometry is then constructed as described below.

From the impeller inlet shape factor and impeller inlet flow coefficient, the optimum blade angle and diameter at the impeller shroud as well as the inlet flow area are evaluated following Rusch and Casey's approach [4]. This method assumes a 0° incidence at the impeller shroud. The hub leading edge is then positioned to maintain the inlet flow area. Both hub and shroud contours are drawn from arcs based on curvature radii suggested by Lüdtke [2].

The impeller outlet width is subsequently derived from the outlet flow coefficient, the impeller outlet diameter and the mass conservation. The outlet flow angle is calculated based on the work input coefficient and the outlet blade angle is retrieved using Wiesner's equation for the flow deviation [11]. Finally, the shroud and hub blade angle distribution suggested by Augnier [1] is followed to generate the final 3D geometry. A trailing edge rake angle of 30° is assumed and a ruled blade is generated by connecting hub and shroud contours. Since only a 3D skeleton geometry is required to fulfil the objective of this study, no thickness distribution is added along the blade camber line.

The stage efficiency is estimated from the impeller design inlet flow coefficient and tip Mach number following the model presented and described first in Casey and Robinson [12]. The correlation is however given in Rusch and Casey [4]. Based on a experimentally obtained performance database of state of the art compressors, this model provides an estimate of the stage performance

at design point without any knowledge on the stage geometry. In fact, unlike other models evaluating separately the different sources of loss (aerodynamic and parasitic losses), a correlation provides directly the stage polytropic efficiency for a given material roughness, Reynolds number, type of diffuser (vaned or vaneless) and impeller (open or closed). Corrections are then applied to obtain the performance to be expected for the case of interest. The off-design performance of the stage is then evaluated using Casey and Robinson's model [13] as well as Casey and Rusch's findings [14] for vaned diffusers. Hence, the compressor performance with vaned diffuser is corrected with respect to its vaneless counterpart at design point and during the off-design performance evaluation. The procedure followed to generate the stage performance map together with its associated impeller 3D skeleton geometry is summarised below.

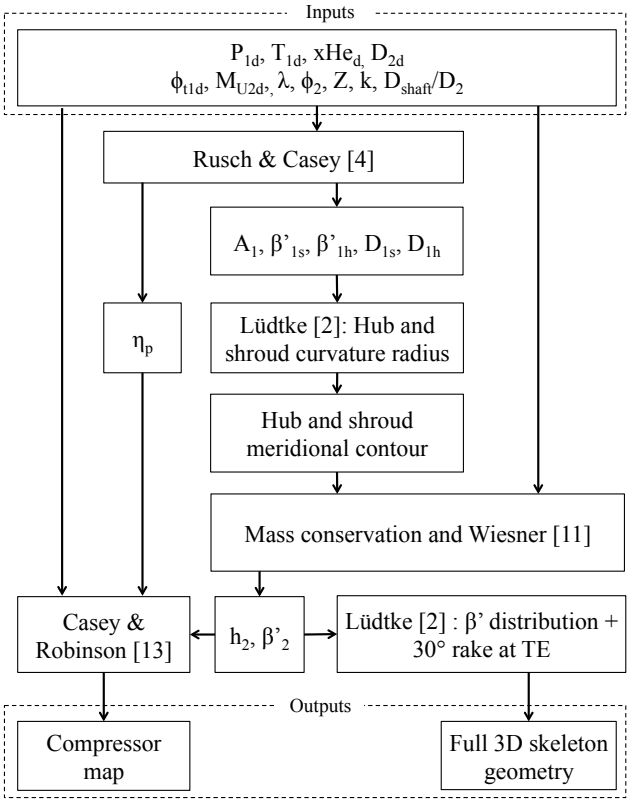

Fig.7 Procedure followed to obtain the stage performance and generate the 3D skeleton impeller design

The generic off-design performance prediction model needs to be tailored to the operation of low pressure ratio impellers. To do so, the model is calibrated using CFD calculations performed for a compressor stage designed at ITSM with the same thermodynamic boundary conditions already mentioned above as well as with a design inlet flow coefficient of 0.07 and a design impeller tip Mach number of 0.53.

The above mentioned CFD calculations as well as the other results discussed below, have been obtained with Numeca Fine^{TM}/Turbo 12.2 [15]. A structured mesh consisting of 1.24 million elements has been used and the Reynolds-Averaged Navier-Stokes (RANS) equations have been closed with the Spalart-Allmaras turbulence model. The same inlet conditions as provided in the impeller design model have been defined, namely total inlet pressure and temperature, and have been set at the inlet boundary of the discretised domain. Additionally, a mass flow rate has been imposed at the outlet section and steady state calculations at several operating points have been conducted for a single passage with vaneless diffuser.

Figure 8 compares the compressor performance map obtained using CFD for various speed lines with the model prediction and measured up to the diffuser outlet plane, highlighting the off-design predictive capabilities of the model after calibration.

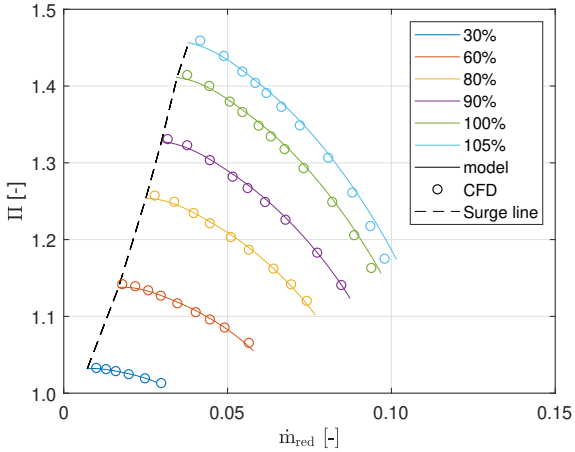

Fig.8 Comparision between CFD results and off-design prediction model after calibration for a nelium compressor

It is worth noting that most calibration coefficients used and presented in Table 1 remain within the ranges suggested by authors [13]. Some of them however, have to be corrected for the performance prediction of low tip Mach number impellers. In fact, the developed model is based on coefficients varying from low to high tip Mach numbers where most of the variation happens justifiably at tip Mach numbers far above the incompressible fluid case. The functions lack of flexibility in the low tip Mach number range can be corrected by modifying the associated coefficients. Since the efficiencies near surge and choke as well as the surge margin have a tendency to be underestimated with the suggested values, D_{low}, $\phi_p/\phi_{c_{low}}$ and $\phi_s/\phi_{c_{low}}$ are corrected. These margins are modified once more for vaned diffusers by taking the values suggested by authors and other coefficients remain constant.

Table 1 Off-design model calibration coefficients

Coeff.	Value	Coeff.	Value	Coeff.	Value
A	1.00	A_s	0	G_{low}	2.00
B	0.85	B_s	1.25	G_{high}	0.30
C	5.00	C_s	4.75		
D_{low}	2.30	$\phi_s/\phi_{c_{low}}$	0.20		
D_{high}	1.70	$\phi_s/\phi_{c_{high}}$	0.84		
H_{low}	2.00	$\phi_p/\phi_{c_{low}}$	0.31		
H_{high}	3.50	$\phi_p/\phi_{c_{high}}$	0.90		

Since the impellers have sensibly different fluid inlet conditions and potentially different impeller outlet diameters than the ones used for their design, the Reynolds number effect has to be taken into account and, in this case, Casey's correction [16] was implemented. This model, similarly to earlier ones such as Strub et al. [17] and Casey [18], follows the approach used in fluid flow to evaluate the friction factor in ducts from the fluid Reynolds number using the Moody diagram. However, the comparison between Casey [16] and earlier models ends at this point since a new unified correction equation is derived from first principles. Moreover, a Reynolds number based on the impeller chord is favoured over a diameter- or exit width-based Reynolds number. The friction coefficients are then directly translated into variation of flow or pressure rise coefficients as well as into efficiency. These results are corrected with empirical coefficients B_{ref}, C_{ref} and D_{ref} dependent on the reference specific speed. To validate the chosen model, additional CFD calculations

are conducted on the above mentioned impeller by varying the inlet pressure with results given in Figure 9 for the 100% speed line.

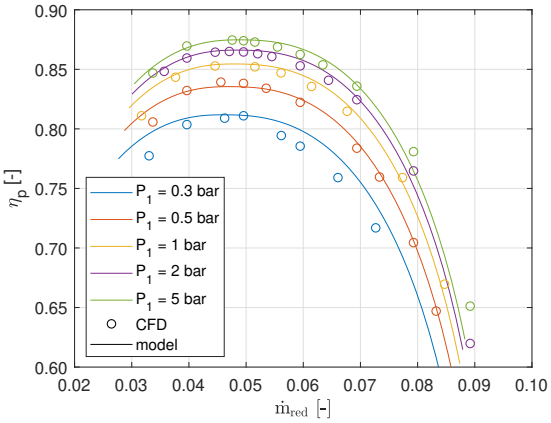

Fig.9 Reynolds number effect on stage performance

As illustrated by this figure, results generated by the model are in good agreement with the CFD calculations even though deviations exist at low inlet pressure, namely at relatively low Reynolds number, as well as at low and high mass flow rate. These deviations were already observed at design conditions but are amplified depending on the Reynolds number. Moreover, as mentioned by Casey [16], the sensitivity of the C_{ref} and D_{ref} coefficients is relatively high for a given reference specific speed. Even though further refinement of these coefficients would help improve the model fit to CFD calculations, stage performance trends seem well predicted overall.

Besides blade scaling, blade trimming is another geometry alteration, that can be applied to any impeller. To leverage industry competences, this study follows a flow trimming methodology. Consequently, the blade is cut from leading edge to trailing edge along a streamline going through the impeller initial geometry and ending at the desired outlet width, as illustrated in Figure 10.

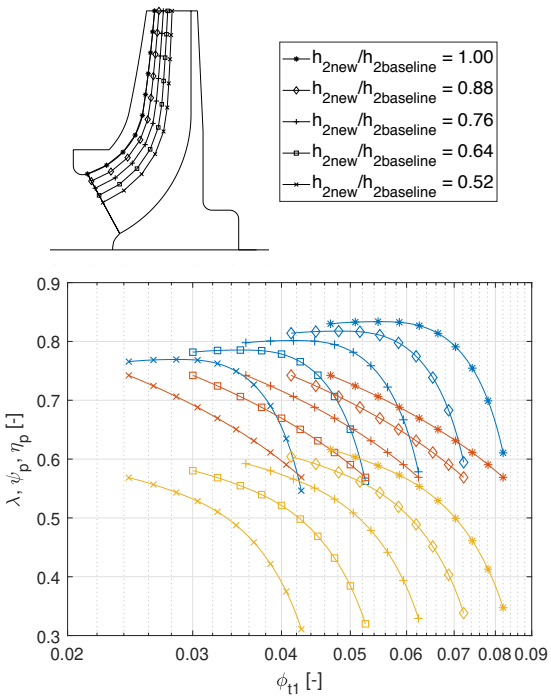

Fig.10 Effect of blade trimming on stage performance

For simplicity, the Root-Mean-Square radius is used to determine the position of the blade cut. Moreover, a choice has to be made between cutting the blade at the hub, at the shroud or at both simultaneously. This choice is usually guided by a trade-off between loss in efficiency and deterioration of rotor dynamics. Figure 10 illustrates the model prediction for the baseline impeller and its variants among a same family with different outlet widths.

MULTI-STAGE STACKING MODEL

Design boundaries to the multi-stage compressor architecture optimisation described below have been set in alignment with industrial design philosophy. First, impellers are chosen from a database following the same restrictions faced by an engineer when selecting the suitable compressor stage among his company database. The relevance of the impeller database size for the multi-stage machine performance and architecture is addressed in the results section.

As per the approach described above, the impeller database regroups parents and families are generated by either scaling, flow trimming from the impeller shroud or a combination of both. Then, a geometry variation by steps is applied to limit the diversity of both impellers within a family and casing geometries. By doing so, the stage manufacturing process is greatly simplified and the stage performance uncertainty reduced. Hence, impellers can be scaled to smaller or larger outlet diameters by 6% steps. The impeller size is also limited by the maximum impeller diameter allowed on the shaft and corresponding motor. Similarly, the impeller can be trimmed from the shroud with an outlet impeller width varying by 6% steps down to a minimum outlet width corresponding to a reduction by a factor close to 2 of the inlet flow coefficient, as illustrated in Figure 10. This discretisation of outlet diameter and outlet width has proven to cover the great majority of application requirements and industry experience shows that intermediary steps are rarely necessary.

Motors with two different maximum rotational speeds of 9'500 and 11'500 RPM are chosen for the design of the multi-stage architecture. Moreover, a range of shaft diameters with minimum and maximum values associated with both motors and the corresponding bearings is also used. Similarly to discretisation methods described above for the impeller outlet width and outlet diameter, the shaft diameters are varied by 5 mm steps. The choice of the final shaft diameter is made knowing the minimum leading edge radius among the impellers mounted on the shaft. An illustration of the possible variations mentioned above are shown in Figure 11. These geometry alterations result in the generation of a so-called impeller family.

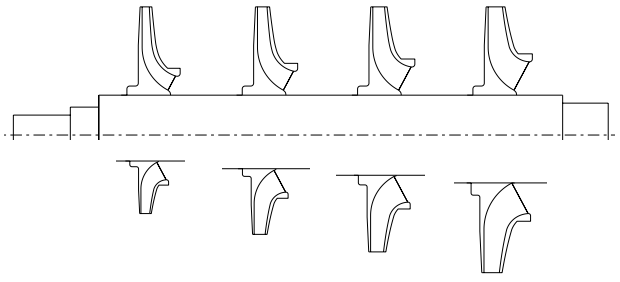

Fig.11 Impeller family generated by blade trimming (top) and impeller scaling (bottom)

The number of impellers per shaft is determined by calibrating the model using results provided by a pre-design tool developed at MAN Energy Solutions Schweiz AG. The latter combines aerodynamic performance evaluation with rotor dynamics validation using the company impeller database. Limitations on the number

of impellers per shaft as well as on maximum impeller tip speeds can be derived from the rotor dynamics evaluation.

Finally, the last design philosophy criterion inspired from industry regards the impeller diameter variation on a specific shaft. For each casing, impeller diameters are kept constant across stages with the exception of the first stage. Since the diameter at this stage varies independently, a higher design flow coefficient impeller can be used to swallow as much flow as possible for the downstream impellers and will also result in a slight increase in overall efficiency. Moreover, this design choice greatly reduces the number of variables compared to a multi-stage machine architecture in which all diameters could vary independently. In the chosen setting with constant outlet diameters, the stage performance of downstream impellers is corrected towards the operating input flow coefficients by impeller trimming.

Furthermore, inputs of the multi-stage stacking model depend on the number of casings and motors. For the first and downstream impellers of each casing, the following inputs are required: the outlet diameter, the design tip Mach number and inlet flow coefficient as well as a coefficient related to the surge margin and used to determine the optimised blade trim. An additional input per motor is required, namely the motor design rotational speed.

These inputs define the multi-stage architecture, whose aerodynamic performance can be evaluated by a stacking method. Hence, the overall performance map per casing can be evaluated using the corrected performance map of each impeller stacked on a same shaft. An example of such design speed lines for a two-casings machine and its architecture is illustrated in Figure 12.

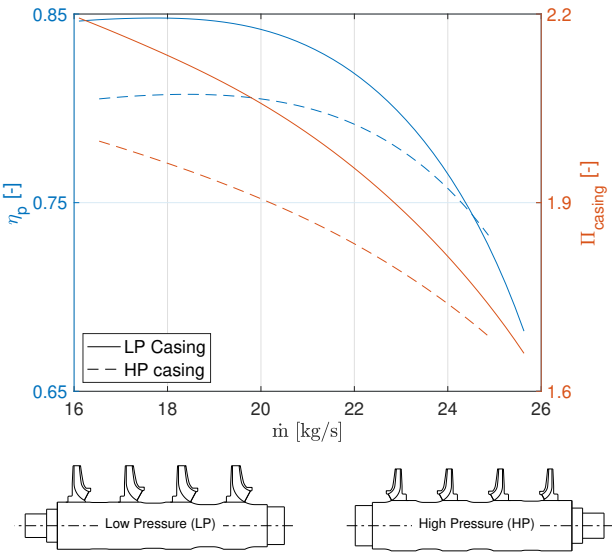

Fig.12 Performance map and associated multi-stage architecture

OPTIMISATION ALGORITHM

As explained above, see Figure 6, two different optimisation loops are required. The first one is connected to the stage performance evaluation model in order to generate optimised geometries for the impeller database. A second one enables to optimise architectures of multi-stage machines. Since both these optimisation problems are global and non-linear, a genetic algorithm is particularly suitable. In fact, while gradient methods perform best when searching for a local optimum, genetic algorithm are particularly adapted when the objective is to find a global optimum.

As vastly described in the literature, genetic algorithms are based on Darwin's theory of evolution relying on the survival of the species with the fittest genome [19]. Hence, coming back to the problem at hand, an impeller with certain design parameters, also referred to as genes, can perform better than one with a different combination of genes. Therefore, the objective of the algorithm is to find the optimal combination of genes leading to the best performing impeller and multi-stage machine architecture. To do so, a population made of several individuals is first created and genes are altered between each generation until a converged solution is found. More details on the theory behind genetic algorithms can be found in many publications such as the one by Goldberg [19].

Hence, both problems follow the same algorithm starting with an initialisation step during which a first population is created. This initial population is generated randomly by applying a normal distribution to the genes around realistic values with standard deviations sufficiently large to cover the widest search space possible.

The population performance is then evaluated based on parameters selected to best characterise the impeller performance. These include: the diffusion along the impeller shroud, also referred to as Haller number DH, the ratio between impeller shroud and outlet diameter D_{1s}/D_2, the ratio between impeller hub and outlet diameter D_{1h}/D_2, the work input coefficient λ, the absolute outlet angle α_2, an estimation of the blade loading BL given by Aungier [1] (see eq. (1)) as well as an estimation of the diffusion factor Deq similar to the one proposed by Lieblein for axial compressors, also provided by the same author [1] (see eq. (2)). Note that the design parameters for this specific application are inherent to subsonic impellers, which explains why the relative Mach number is not monitored here.

$$BL = \frac{2\Delta W}{W_1 + W_2} \tag{1}$$

$$Deq = W_{max}/W_2 = \frac{W_1 + W_2 + \Delta W}{2W_2} \tag{2}$$

Where $\Delta W = 2\pi D_2 U_2 \lambda / (Z L_B)$ and L_B is the mean camber line length.

With regard to the multi-stage architecture optimisation, the following parameters are evaluated and monitored: outlet discharge pressure P_{out}, overall machine efficiency η and operating margin at design speed OM.

Based on these performance parameters, a fitness function is derived. To do so, each performance parameters are associated with a penalty of the following form in alignment with the approach described by Casey et al. [20] and implemented in commercial software [15]:

$$P = \left(\frac{Q - Q_{req}}{Q_{ref}} \right)^n \tag{3}$$

Where Q is the calculated quantity, Q_{req} its required value and Q_{ref} a reference value used to normalize the penalty. As suggested in the literature, the exponent n is set to 2.

Alternative expressions are used depending on the objectives associated with each performance parameter. These could simply be to maximise/minimise in absolute (referred to as type 1) or until a certain value (referred to as type 2) the parameter value or to maintain it within a certain target range (referred to as type 3). For both optimisation problems, all performance parameters mentioned previously are given in Table 2 together with penalty function types (i.e. 1, 2 or 3), objective values and reasons for choosing these parameters.

Table 2 Performance parameters and associated penalty functions

Param.	Type	Value	Reason
Impeller optimisation			
DH	2	≥ 0.70	Minimise flow separation
D_{1_s}/D_2	3	≥ 0.40 ≤ 0.75	Minimise losses
D_{1_h}/D_2	3	≥ 0.35 ≤ 0.50	Shaft stiffness
λ	1	Maximise	Maximise pressure rise
α_2	3	$\geq \alpha_{2_{obj}} - 1°$ $\leq \alpha_{2_{obj}} + 1°$	Minimise losses through diffuser
Deq	2	≤ 1.70	Reasonable surge margin
BL	2	≤ 0.90	Reasonable blade loading
N	1	Minimise	Minimise polar inertia
Multi-stage architecture optimisation			
η	1	Maximise	Maximise efficiency
P_{out}	3	$\geq P_{out_{obj}}$ $\leq P_{out_{obj}} + 1$ bar	Required pressure rise
OM	2	≥ 0.35	Required minimum OM

The weighted sum of all penalties is then calculated following equation (4). The fitness function representing the overall penalty is subsequently minimised.

$$F = \sum_{i=1}^{nbr\ penalties} w_i P_i \tag{4}$$

Following this evaluation process, a selection is made within the population to identify the parents of the next generation. A crossover and mutation process are thus required to construct this new generation. On the one hand, during the crossover step, also called reproduction, genes are exchanged between individuals. On the other hand, during the mutation process, specific genes of individuals can mutate and vary within a certain range. For each of these processes, different methods have been implemented and tested. These are listed below for completeness. More information on these models as well as additional ones can easily be found in the literature (e.g. Goldberg [19] or Mühlenbein and Schlierkamp-Voosen [21]).

Selection: Uniform, truncation, tournament and roulette wheel
Crossover: Single points, two points, uniform and half uniform discrete, extended intermediate recombination (EIR), extended line recombination (ELR)
Mutation: Power law uniform distributed and normal distributed

The different selection, crossover and mutation methods have been implemented and tested to study their effect on the convergence rate and the capacity of finding a global optimum among many local optima. Methods leading to what is commonly referred to as a Breeder Genetic Algorithm (BGA) [21] are then applied to both optimisation problems. Hence, a truncation selection, a normal distributed mutation and an extended line recombination are used. Alternative algorithms such as Adaptive Genetic Algorithm (AGA) have also been analysed but proved to be less effective for such optimisation problems.

In addition, a scaling of the fitness function is implemented to ensure that the algorithm does not converge too rapidly towards a local optimum. This could be the case when individuals, which seem initially weak, are disregarded although they could have provided genes leading to an optimised solution at a later stage. Hence, this scaling of the fitness function enables to maintain a diversity among the pool of candidates. The raw fitness function can be scaled following different distributions such as linear, power law, exponent law or sigma. After having tested these different methods, the linear scaling appeared be the most effective for the impeller optimisation and the exponent law for the multistage architecture optimisation. An elite selection was also implemented to ensure that the best individual found in previous iterations is kept from one generation to another.

Finally, a hill climbing process is initiated as soon as either no more reduction of the fitness function is observed from ite_{check} iterations on or after a certain number of iterations. This process enables to realise the latest incremental improvements by focusing on the near vicinity of the last result obtained and thus to reach the global optimum of the fitness function. This algorithm and the different processes mentioned above are summarised in Figure 13.

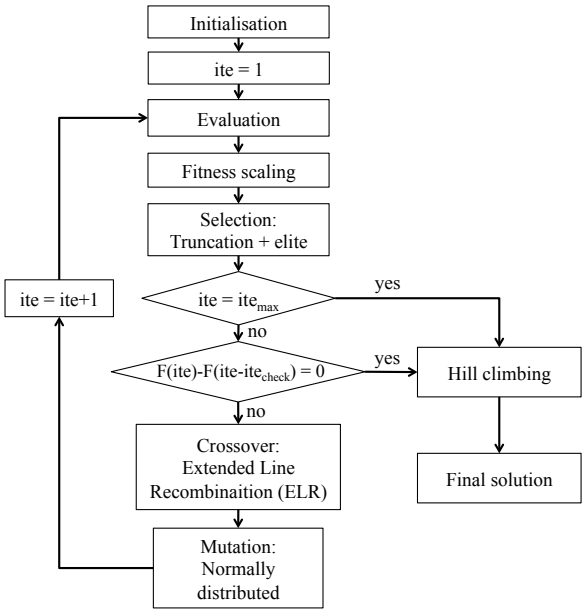

Fig.13 Genetic algorithm

RESULTS

Impeller database generation

To generate an impeller database covering the needs of all gas mixtures, impellers have been designed with following design parameters: design flow coefficients between 0.01 and 0.11 with 0.005 steps and for impeller tip Mach numbers between 0.1 and 0.7 with 0.05 steps. A meridional view of the results obtained with this optimisation is given in Figure 14 for a design tip Mach number of 0.4. The database generated enables to select the optimum impeller design enhancing the performance of the multi-stage architecture.

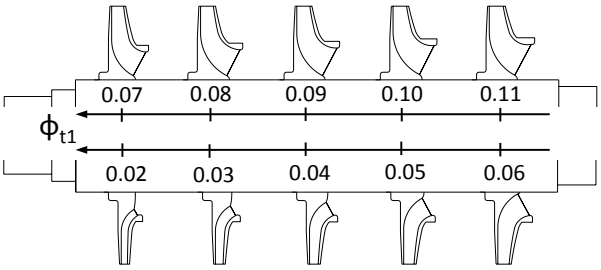

Fig.14 Impeller geometry variation with respect to the design inlet flow coefficient

Figures 15 provides an overview of the performance and geometrical parameters of impellers constituting the database for a design tip Mach numbers of 0.4. Hence, the stage polytropic efficiency obtained from Rusch and Casey's expression [4] for a low tip Mach number is displayed together with the predicted polytropic pressure

coefficients. When looking at the literature, these distributions of performance parameters are in good agreement with the ones provided by Aungier [1].

Moreover, it can already be deduced that a trade-off between machine efficiency and total number of stages exists. In fact, on the one hand, for a low amount of stages satisfying the total pressure ratio requirement, impeller diameters will have to be maintained as high as possible, constraining the inlet flow coefficient to decrease rapidly between stages together with the efficiency per stage. On the other hand, for a higher amount of stages, the impeller diameters can be reduced more severely from one casing to another. This results into impellers with design inlet flow coefficients maintained at a higher average level, thus leading to higher overall machine efficiencies.

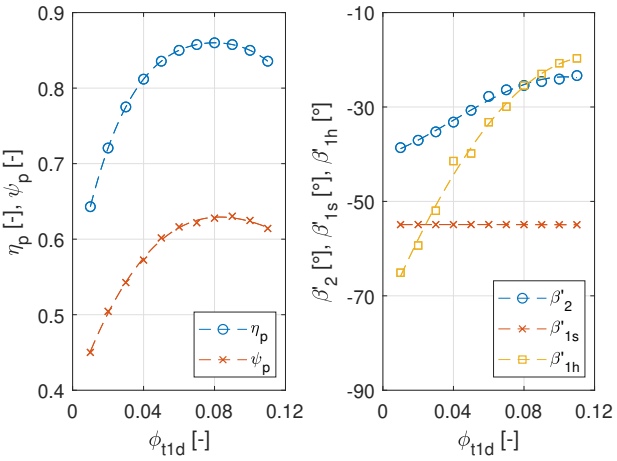

Fig.15 Performance (on the left) and geometrical (on the right) parameters of impellers within the database for $M_{U_2d} = 0.4$

Since all the designs of interest are for tip Mach numbers below 0.8, the stage performance does not vary with this design parameter and only depends on the inlet flow coefficient. Moreover, designing impellers for these high speed of sound gases also explains the comparatively low shroud inlet blade angle β'_{1s} in comparison to the more conventional air impellers. In fact, as explained by Rusch and Casey [4], by assuming a zero incidence at the impeller shroud, an optimal blade angle can be determined resulting in a minimum inlet relative Mach number M_{w1} and thus, lower losses explained by a lower diffusion along the impeller shroud.

To do so, an expression for a modified mass flow function resulting in equation (5) is derived and written with respect to the impeller inlet relative Mach number and shroud flow angle:

$$\frac{4\phi_{t1}M_{U_2}^3}{k\pi} = \frac{M_{w1}^3 \sin^2\beta_{1s}\cos\beta_{1s}}{\left[1+\frac{\gamma-1}{2}M_{w1}^2\cos^2\beta_{1s}\right]^{1/(\gamma-1)+3/2}} \quad (5)$$

This function is plotted in Figure 5 of Rusch and Casey [4] for different inlet relative Mach numbers and shows that for each modified flow coefficient a minimum inlet relative Mach number can be determined with an optimal inlet fluid angle. Moreover, for low inlet relative Mach numbers such as for light gases application, the second term of equation (5) can be reduced to $\tan^2(\beta_{1s})$. Hence, in this specific case, the function maximum corresponding to the minimum inlet relative Mach number is reached at $\beta_{1s} = 54.74°$. This result can be observed in Figure 16, where the impeller shroud inlet solid angle is displayed for different tip Mach numbers. Passed the design cases with the highest gas speed of sound, the absolute value of this angle increases mainly with the tip Mach number but the influence of the design inlet flow coefficient also grows in magnitude.

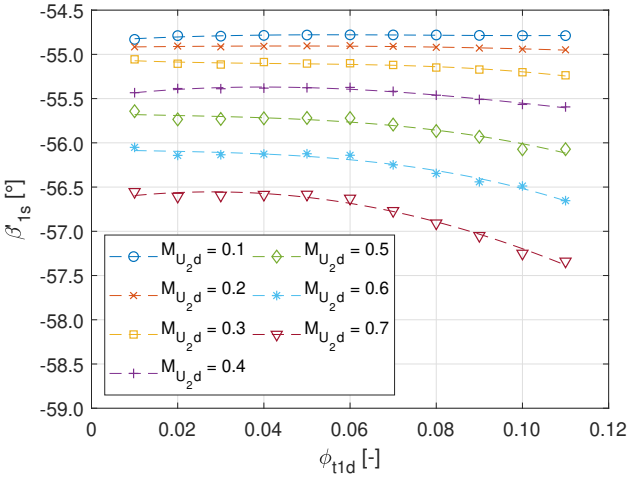

Fig.16 Influence of impeller design tip Mach number and inlet flow coefficient on impeller inlet shroud angle

Moreover, since the inlet shape factor increases with the design inlet flow coefficient, the hub diameter is also reduced as it can be seen in Figure 14. This also results in short and large diameter shaft for the low flow coefficient impellers and thinner and longer shaft for the high flow coefficient impellers. This observation also implies that the absolute hub blade angle decreases for higher flow coefficients in order to compensate for the lower rotational speed while maintaining a reasonable flow incidence (see Figure 15).

Finally, the absolute outlet blade angle also has a tendency to decrease as the inlet flow coefficient increases. In fact, by increasing the design inlet flow coefficient at a constant impeller tip speed, the outlet blade angle has to be reduced if the objective is to maintain a high work input coefficient maximising the pressure rise per stage.

Multi-stage architecture at a fixed gas composition (xHe = 0.5)

Results of the multi-stage architecture optimisation are first presented for a constant operating gas mixture with a helium mole fraction of 0.5 and then for the whole gas mixture range. Starting with a constant operating gas mixture, the convergence of the multi-stage architecture optimisation is illustrated below. This calculation aims at maximising both the efficiency and the operating margin. Moreover, penalties associated to these parameters are also provided. As expected, results show that the efficiency and operating margin progressively increase with iterations while their associated penalties decrease. Additionally, the penalty associated with the discharge pressure enables to keep the latter inside the desired range.

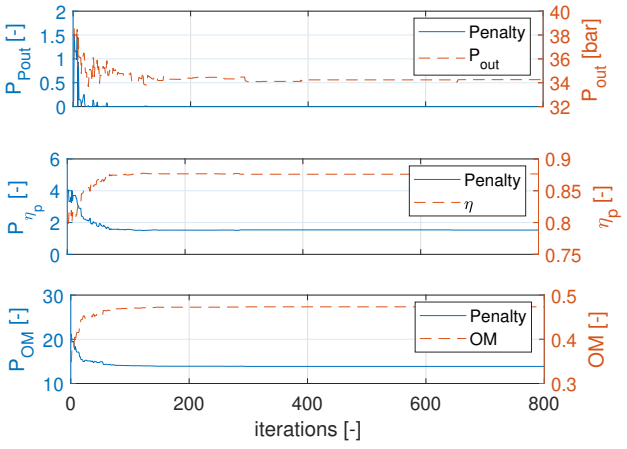

Fig.17 Convergence of the multi-stage architecture optimisation

Following the same optimisation calculation as shown in Figure 17, the population performance evolves through iterations until it hits a Pareto front trading efficiency for range (see Figure 18).

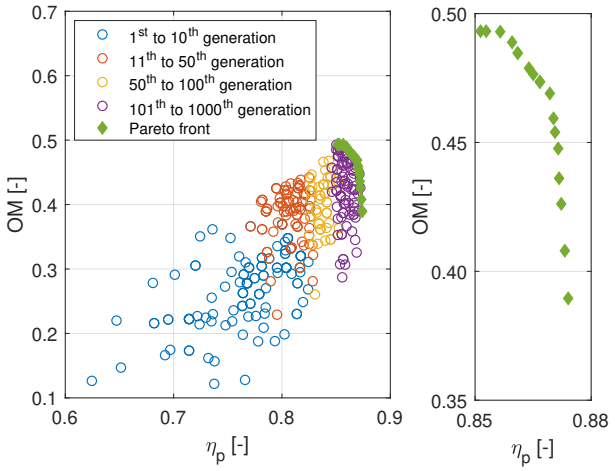

Fig.18 Pareto front between efficiency and operating margin

In order to understand the factors influencing the previously mentioned performance parameters, an impact analysis of the model inputs is conducted using optiSLang [22]. Since only the overall machine efficiency could be predicted in a short time using a polynomial model leading to reasonable accuracy (i.e. above 90% of Coefficient of Prognosis (CoP)), only the effect of the input parameters on the latter is analysed. A comparable accuracy could be obtained for the operating margin but required time consuming models. The analysis was conducted for architectures designed at seven different gas mixtures between pure helium and pure neon each time with a sample size greater than 3'000. Figure 19 displays the average CoP of the input parameters for a representative case obtained at xHe = 0.5. The same order of importance between input parameters is observed for other gas mixtures.

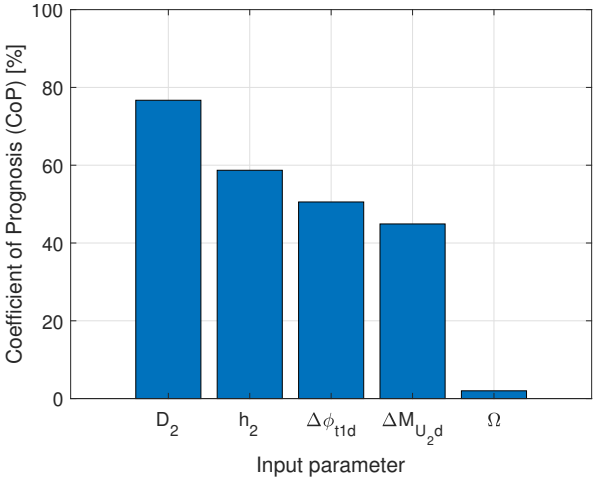

Fig.19 Impact of input parameters on overall machine efficiency

These results are inherent to the approach followed in the multi-stage optimisation model as well as to the strong relation between inlet flow coefficient and stage efficiency. In fact, in order to select impellers with suitable design inlet flow coefficient and tip Mach number from the database, a distribution of these parameters through the machine is first estimated using the impeller diameters and shaft rotational speed. Variations of inlet flow coefficient and tip Mach number can then be added using two of the model input parameters, namely $\Delta\phi_{t1d}$ and ΔM_{U_2d}. Moreover, since the inlet flow coefficient evolves with D_2^3 but is only proportional to $1/\Omega$ a step change in impeller diameter has a comparatively stronger impact on the flow coefficient than a change in rotational speed. However, for heavier gas application, a more pronounced impact of the rotational speed would be anticipated due to the tip Mach number effect on the stage efficiency.

The second parameters influencing strongly the efficiency is the one defining the reduction of impeller outlet width due to blade trimming. Its effect on the stage performance and consequently on the overall machine efficiency can be easily explained by the performance correction illustrated in Figure 10.

Finally, the effect of a variation of design inlet flow coefficient and tip Mach number on the machine overall efficiency results mainly from an off-design drop in stage efficiency. In addition, the variation of design inlet flow coefficient also impacts the stage efficiency at design point. This is however not the case for the tip Mach number since the latter is too low for this specific application to have any effect on the stage performance at design point.

As previously explained, these first optimisations aim at maximising both the efficiency and the operating margin. However, since the operating margin is not critical for the application under study, only the efficiency is now maximised and a minimum operating margin is defined (Table 2). The impact of this constraint on the operating margin and of the number of stages on efficiency is shown in Figure 20.

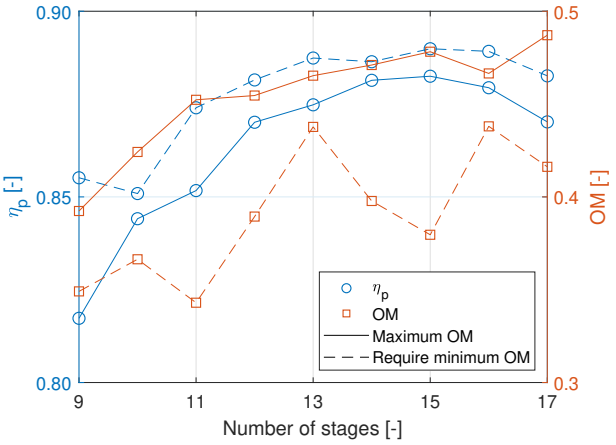

Fig.20 Effect of the operating margin constraint and the number of stages on overall efficiency

As already illustrated by the Pareto front, removing the operating margin maximisation constraint leaves some room for improvement of the efficiency. Hence, regardless of the number of stages, the overall machine efficiency at a maximised operating margin is always lower than the one at an operating margin set above a specific threshold. Moreover, for both optimisation objectives, it can be observed that adding more stages contributes to increasing the overall machine efficiency but only up to a certain value. Pass this limit, adding additional stages penalises efficiency but can still improve the operating margin further.

The number of available impeller families also impacts the machine performance and architecture. Figure 21 displays the overall machine efficiency evolution as the number of impeller families used in architectures increases. Results are given for architectures providing the required discharge pressure, i.e. machines constituted of 9 to 13 stages.

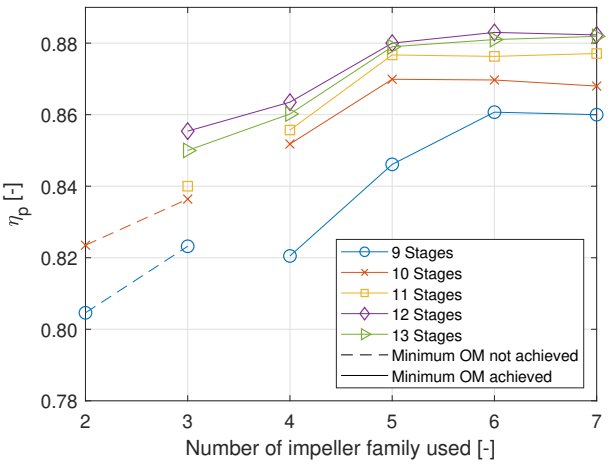

Fig.21 Effect of the impeller family variety on overall efficiency

Firstly, it can be observed that a too small number of impeller families does not guarantee the minimum required operating margin. Once the first configuration respecting the constraint on the operating margin is identified, the overall machine efficiency progressively increases with the number of impeller families. Hence, instead of designing the machine with a limited number of impeller families and thus relying on blade trimming to obtain the right flow coefficient, increasing the number of available families enables to provide each stage with an impeller designed as close as possible to the machine operation requirement. This improved efficiency reaches its limit above a certain number of families, stays roughly constant and can even decrease if a too diverse set of impellers is used. This decrease in efficiency after a certain number of impeller families is strongly correlated with the discretisation of the design inlet flow coefficient and tip Mach number inside the database. In fact, by forcing the multi-stage architecture to include a high amount of different impeller families in comparison with the impeller diversity of the database, suboptimal impellers are placed in the architecture. As a result, from an efficiency perspective, it is recommended to define an optimal number of impeller families above which no additional gain in overall efficiency is observed.

When one compares different architectures with different number of stages at a constant number of impeller families, results similar to the ones presented in Figure 20 can be observed. In fact, the overall machine efficiency improves as the number of stages increases. However, the incremental efficiency decreases until adding more stages does not contribute anymore to the overall machine efficiency and even leads to its deterioration. This could be replicated for other gas mixtures and therefore, an optimised multi-stage architecture can also be obtained in order to either:

- minimise the number of required stages, risking to compromise the overall efficiency, or
- maximise the overall efficiency, risking to require several additional stages.

Multi-stage architecture: from pure helium to pure neon

The following section focuses on the results obtained for the whole gas mixture range, i.e. from pure helium to pure neon. Firstly, as already mentioned, multi-stage architectures can be optimised to either minimise the number of required stages or maximise their overall efficiency while maintaining a reasonable operating margin. Figure 22 highlights the difference in number of stages between these two optimisation objectives for the gas mixtures of interest. The first observable trend is that, whatever the objective, the number of required stages increases with higher content of helium following a quadratic distribution with a sharp increase in the required number of stages above a 0.5 helium mole fraction. This observation was already foreseen in the pressure ratio per stage estimation given for different gas mixtures in Figure 4. This result also explains the current difficulty of turbomachine manufacturers to design a sealed, compact and economically affordable machine for pure helium due to the high number of required stages associated with this application.

Another observation, which can be inferred from Figure 22, is that the architecture with the highest overall efficiency requires the highest number of stages and significantly more so at high content of helium compared to architectures with minimum number of stages. Therefore, at pure helium a significant number of stages has to be added, in comparison to the pure neon case, to reach the highest efficiencies. Designing a multi-stage turbocompressor respecting the target discharge pressure is already costly and financial challenges are accentuated for heavier operating gases if the objective is to design a highly efficient machine.

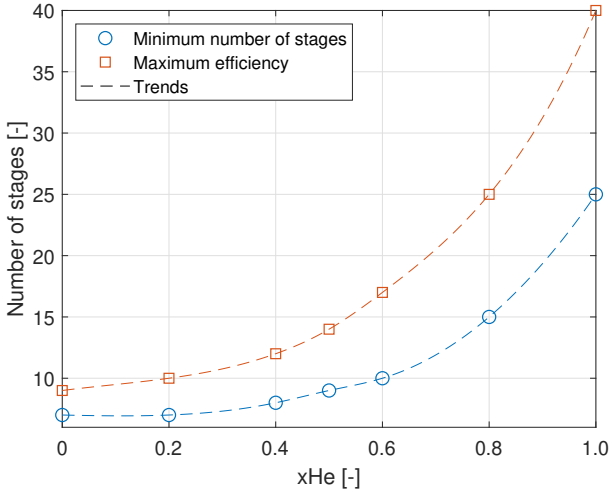

Fig.22 Required number of stages with respect to the helium mole fraction

To explain the variations in number of stages and efficiencies between different gas mixtures, it is worth looking at the design impeller inlet flow coefficients and tip Mach numbers chosen for the different architectures. Figure 23 shows for several gas mixtures the average value of the previously mentioned parameters per architecture when the required number of stages is minimised.

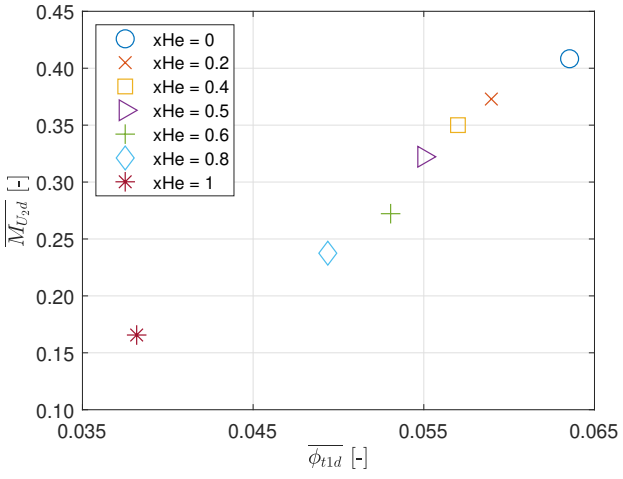

Fig.23 Average ϕ_{t1d} and M_{U_2d} in multi-stage machine architecture for different operating gas compositions

As expected, the design impeller tip Mach numbers chosen for the architectures decreases as the gas becomes lighter and the gas speed of sound increases. Moreover, the inlet flow coefficients also decrease as the mole fraction of helium increases. This is caused by a lower operating mass flow rate for pure helium than for pure neon operation and cannot be compensated by the impeller diameter or rotational speed due to the objective of maximising the pressure rise per stage.

Another particularly important aspect to consider is the effect of impeller database limitations on the performance of the overall machine. The results discussed above have been obtained using a relatively diversified impeller database with a wide range of design tip Mach numbers and inlet flow coefficients. Hence, Figure 24 compares the minimum number of required stages obtained using the diversified impeller database with the ones obtained using two databases containing impellers designed for respectively a pure neon ($M_{U_2d} = 0.4$) and a heavier hypotetic monoamotic gas ($M_{U_2d} = 0.7$) application. Moreover, both databases include six impellers designed for input flow coefficients between 0.02 and 0.09.

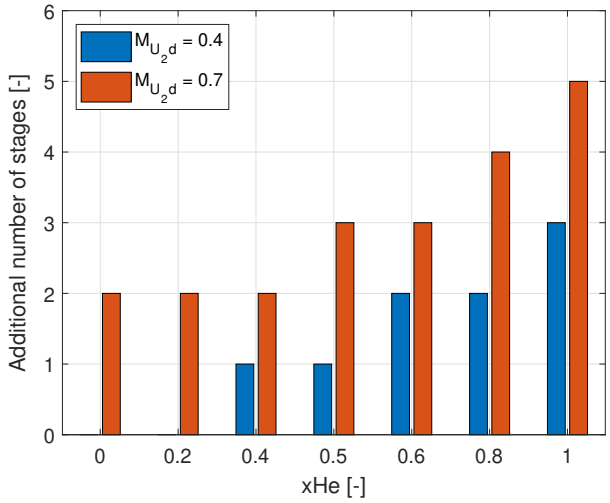

Fig.24 Effect of available impellers on the number of stages

As illustrated by Figure 24, having an impeller database designed for gases with molecular weights deviating greatly from the operating gas, significantly impacts the multi-stage architecture. For instance, selecting only impellers with tip Mach numbers characteristic of pure neon ($M_{U_2d} = 0.4$) to be part of a new database leads to an architecture with three additional stages when the machine is operated with pure helium. This effect is emphasised when the database is optimised for even heavier gases. Moreover, the two databases are designed at constant tip Mach numbers but the multi-stage machines are stacked with impellers operating within a range around the average tip Mach numbers given in Figure 23. This restricted flexibility in the available M_{U_2d} as well as ϕ_{t1d} also contributes to needing additional stages. Figure 24 thus highlights the need of using impellers with suitable design tip Mach numbers tailored to the operating gas, especially when the objective is to reduce the number of required stages.

The last effect of interest comes from potential technological improvements, which can be anticipated in the near future. Among these, the access to lighter materials or the development of motors both with increased maximum rotational speeds and maintained high input power are particularly promising. These technological advancements would enable to reach higher impeller tip speeds. Higher maximum rotational speeds and increased maximum allowable impeller tip speeds constrained by the rotor dynamics result in variations of the multi-stage architecture as illustrated in Figure 25.

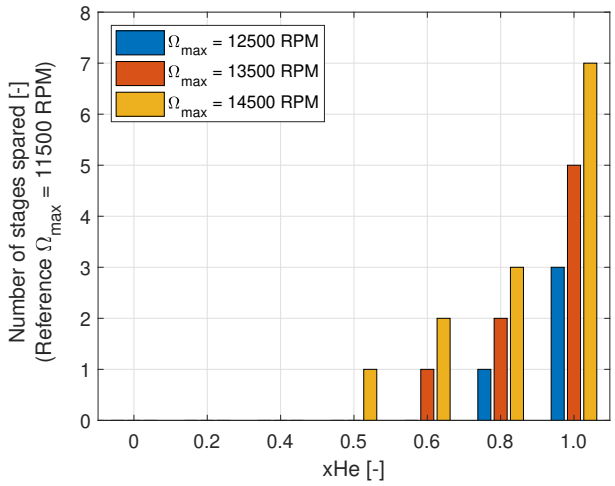

Fig.25 Effect of the maximum motor rotational speed on the number of stages

It can be noted that this impact appears for gases with a helium mole fraction above 0.5. Beyond this threshold, increasing the maximum rotational speed enables to reduce the required number of stages. Consequently, this effect becomes more pronounced as the the gas density is reduced. All in all, the highest the maximum rotational speed unlocked by technological progress, the strongest the potential improvements in multi-stage architecture compactness.

CONCLUSIONS

This paper takes the industrial perspective of multi-stage turbocompressor design and applies it to a light gas application (i.e. a mixture of helium and neon) resulting from CERN's specifications for the new cryogenic cycle of their Future Circular Collider. Hence, a stage performance prediction and a stage stacking model are coupled to a same optimisation algorithm in order to build an impeller database and design a multi-stage machine at a specific gas mixture. A model predicting the performance correction of a scaled or trimmed impeller is also implemented. Design boundary conditions observed in industry and resulting from design philosophies, impeller material or manufacturing techniques available as well as rotor dynamics limitations are taken into account.

The stage performance and geometry of impellers constituting the database is first presented and compared to the literature for different design flow coefficients and tip Mach numbers. Results of the multi-stage design optimisation are then described for a specific gas mixture together with the Pareto front leveraging efficiency for range. The influence of the different parameters defining the architecture on the overall machine efficiency is also analysed. Then, results show that an optimal number of stages for either the most compact or efficient machine can be determined. Moreover, for a given gas mixture, the diversity of impeller family in the machine architecture also contributes to its overall performance. Thus, a minimum number of family is required to achieve the minimum desired operating range. Imposing a stronger diversity leads to an increase in overall machine performance until an excess in diversity becomes detrimental. Results are then provided for the whole range of gas mixture, highlighting how the number of required stages increases exponentially with helium content. As the gas becomes lighter, the average machine flow coefficient and tip Mach number also decrease. The available impeller in the database as well as the foreseen technological improvements greatly influence the final multi-stage architecture. Relying on a compressor database with a limited number of design flow coefficients and optimised for heavier gases than the application requires leads to less compact architectures in comparison to a machine with fully tailored-design

stages. Finally, enhancing the motor performance by increasing its maximum rotational speed together with its rated power also contributes to reducing the required number of stages especially for high helium content.

In future work, several improvements of the models would help make the latter suited for a wider range of applications. The multi-stage design model would gain in additional degrees of freedom by implementing different ways of impeller trimming together with their effect on the stage performance. Moreover, it would be worth extending the models to heavier gases such as air or even heavy gas mixtures such as the ones encountered in the oil and gas industry. A performance correction capturing the change in specific heat ratio would also come fine tune the model prediction. This would enable to further validate the results with existing multi-stage machines.
An experimental validation of the off-design model using an industrial compressor stage with vaned diffuser and designed for light gases is also scheduled for the near future. The coefficients responsible for the surge and choke margins prediction could therefore be calibrated for this specific application instead of being restricted to the literature-recommended values.
Furthermore, one limitation of the current model is the inherent link with the baseline machine used. Even if MAN Energy Solutions experience with the HOFIM^{TM} architecture enables to provide design boundaries such as limitations for the required number of stages and maximum impeller tip speeds, it also restricts the application to this specific machine. This limitation could be lifted by implementing a model directly connecting shaft and impeller geometry as well as rotational speed to the allowable number of stages per shaft. Moreover, by doing so, the impeller database would be comprised of geometries optimised not only for aerodynamic performance but also for rotor dynamics restrictions. Finally, with such a model taking into account the effect of impeller material on the rotor dynamics, a more accurate estimation of the gain coming from technological improvements would be possible.

ACKNOWLEDGMENTS

The valuable technical discussions and email exchanges with Chirstoph Andris and Dr. Bob Mischo from MAN Energy Solutions are gratefully acknowledged. Moreover, the first author would like to thank MAN Energy Solutions for having provided in house resources and tools as well as valuables informations on their products and engineering experience. Finally, the author would also like to thank the ITSM for providing the computing tools and the Marie Skodolwska-Curie Action (MSCA) for its financial support, which made this work possible.

EASITrain - European Advanced Superconductivity Innovation and Training. This Marie Sklodowska-Curie Action (MSCA) Innovative Training Networks (ITN) has received funding from the European Union's H2020 Framework Programme under Grant Agreement no. 764879

References

[1] Aungier, R. H., 2000, "Centrifugal Compressors - A Strategy for Aerodynamic Design and Analysis", ASME, New York.

[2] Lüdtke, K. H., 2004, "Process Centrifugal Compressors", Springer, Berlin.

[3] Dixon, S. L., 2005, "Fluid mechanics and thermodynamics of turbomachinery, 5th edition", Butterworth-Heinemann, Oxford.

[4] Rusch, D. and Casey, M., 2013, "The Design Space Boundaries for High Flow Capacity Centrifugal Compressors", *Journal of Turbomachinery*, Vol. 135.

[5] Casey, M. V., and Schlegel, M., 2010, "Estimation of the Performance of Turbocharger Compressors at Extremely Low Pressure Ratios," *Proceedings of the Institution of Mechanical Engineers, Part A: Journal of Power and Energy*, Vol. 224, pp. 239–250.

[6] Dalbert, P., Casey, M.V., and Schurter, E., 1988, "Development, testing and performance prediction of radial stages for multi-stage industrial Compressors", *Journal of Turbomachinery*, Vol. 110, pp. 283-292.

[7] Dalbert, P., Ribi, B. and Casey, M. V., 1999, "Radial compressor design for industrial compressors", *Proceedings of the Institution of Mechanical Engineers, Part C: Journal of Mechanical Engineering Science*, Vol. 213, pp. 71-83.

[8] Al-Busaidi, W., and Pilidis, P., 2016 "A new method for reliable performance prediction of multi-stage industrial centrifugal compressors based on stage stacking technique: Part I – existing models evaluation", *Applied Thermal Engineering*, Vol. 98, pp. 10-28.

[9] Al-Busaidi, W., and Pilidis, P., 2015, "A new method for reliable performance prediction of multi-stage industrial centrifugal compressors based on stage stacking technique: Part II–New integrated model verification", *Applied Thermal Engineering*, Vol. 90, pp. 927-936.

[10] Romei, A., Maffulli, R., Sanchez, C. G., and Lavagnoli, S., 2017, "Design and Optimization of Multi-Stage Centrifugal Compressors With Uncertainty Quantification of Off Design Performance", ASME Turbo Expo 2017.

[11] Wiesner, F. J., 1967, "A review of slip factors for centrifugal impellers", *Journal of Engineering for Power*, Vol. 89, pp. 558-566.

[12] Casey M.V., Robinson C.J., 2006, "A guide to turbocharger compressor characteristics", *Dieselmotoren- technik*.

[13] Casey, M. and Robinson, C.J., 2013, "A Method to Estimate the Performance Map of a Centrifugal Compressor Stage", *Journal of Turbomachinery*, Vol. 135.

[14] Casey, M. and Rusch, D., 2014, "The matching of a vaned diffuser with a radial compressor impeller and its effect on the stage performance. Journal of Turbomachinery", Vol. 136.

[15] NUMECA International, 2009, "FINE/Turbo v8. 7, user manual", Brussels.

[16] Casey, M. V. and Robinson, C. J., 2011, "A unified correction method for Reynolds number, size, and roughness effects on the performance of compressors", *Proceedings of the Institution of Mechanical Engineers, Part A: Journal of Power and Energy*,Vol. 225, pp. 864–876.

[17] Strub, R. A., et al., 1987, "Influence of the Reynolds Number on the Performance of Centrifugal Compressors", *ASME Journal of Turbomachinery*, Vol. 109, pp. 541-544.

[18] Casey, M.V., 1985, "The effects of Reynolds number on the efficiency of centrifugal compressor stages", *Journal of Engineering for Gas Turbines and Power*, Vol. 107, pp. 541-548.

[19] Goldberg, D.E., 1989, "A genetic Algorithms in Search, Optimisation and Machine Learning", Addison, Wesley.

[20] Casey, M.V., Gersbach, F., and Robinson, C.J, 2008, "A new optimisation technique for radial compressor impellers", ASME Turbo Expo 2008.

[21] Mühlenbein, H., and Schlierkamp-Voosen, D., 1993, "Predictive models for the breeder genetic algorithm", *Evolutionary computation*, Vol. 1, pp. 25-49.

[22] DYNARDO GmbH, 2012, "Methods for multi-disciplinary optimization and robustness analysis", Weimar.